Journal of the Korean Physical Society, Vol. 66, No. 6, March 2015, pp. 952∼958

Super-fast Switching of Twisted Nematic Liquid Crystals with a Single-wall-carbon-nanotube-doped Alignment Layer

Yang Liu
Department of Electrical and Electronic Engineering, Yonsei University, Seoul 120-749, Korea

Young Jin Lim, Sudarshan Kundu and Seung Hee Lee*
Applied Materials Institute for BIN Convergence,
Department of BIN Fusion Technology and Department of Polymer-Nano Science and Technology,
Chonbuk National University, Jeonju 561-756, Korea

Gi-Dong Lee†
Department of Electronics Engineering, Dong-A University, Busan 604-714, Korea

(Received 26 November 2014, in final form 29 December 2014)

The application of a single-wall carbon-nanotube (SWCNT) and polyimide (PI) composite thin film on an indium tin-oxide (ITO) glass substrate, working as the command surface in a twisted nematic liquid crystal display (LCD), is described. SWCNTs were chopped and oxidized in a strong acid medium to make them more miscible in a polyimide solution. A film of this newly-developed PI-SWCNT composite was rubbed to determine the director direction for the LC molecules. The newly-fabricated command surface was examined using a laser beam profiler and atomic force microscopy. Sizes of shortened SWCNTs were characterized by using field-emission scanning electron microscopy (FE-SEM). Finally, small-sized test panels were fabricated from this composite-coated ITO glass, and their electro-optic performances were measured. Although the operating voltage to switch a cell was increased by around 41%, the switching speed was improved remarkably. The rise time of the test cells was found to be improved by around 10.12% and the decay time by around 29.77%. Thus, an overall improvement of around 16.12% in the total switching time was achieved. The change in the surface morphology of the newly-developed composite materials was found to be one of the factors responsible for the faster switching of the device. Detailed discussions are given in this report to explain the faster switching of the newly-developed twisted nematic liquid crystal display (TN-LCD). The device can be useful for practical applications.

PACS numbers: 71.20.Tx, 42.70.Df
Keywords: Liquid crystal display, CNT, Nanocomposite, Alignment layer
DOI: 10.3938/jkps.66.952

I. INTRODUCTION

Nowadays, liquid crystal displays (LCDs) are the most widely used display devices and LCDs are still being developed. Considering the numerous material issues and technology problems raised in meeting market demands, engineers are still hunting for new modes, new materials, or new technologies [1–6] with better performance, such as faster response time, wider viewing angle, higher contrast ratio, and so on. Liquid crystals (LCs) are optically anisotropic liquids, and they can effectively change or control the state of polarization of light passing through them. This property has been successfully used to make display devices. To use that property purposefully, one needs to control the direction of the nematic LC molecules in a device, and in order to control the director's orientation, one needs to use a proper modification to align the molecules homogeneously in a plane vertical to the substrate. This surface is often called the command surface. Hence, alignment layer development has been one of the most important ares for decreasing the response time of LCDs because of its advantage of low power consumption and high reliability [7]. Two major approaches are used to decrease the response time of LC molecules and to decrease the driving voltage of a cell with an alignment layer [8]; one is controlling the pretilt angle of the LC molecules by using chemical or physical methods, and the other is manipulating the capacitance of the alignment layer such that the accumu-

*E-mail: lsh1@chonbuk.ac.kr; Fax: +82-63-270-2341
†E-mail: gdlee@dau.ac.kr

lated volume charge induces a polarization field on the LC. Until now, few attempts in which carbon nanotubes (CNTs) have been used to decrease the response time effectively, such as doping CNTs in LCs directly [9–11], doping CNTs in the alignment layer [8] or in the carbon-nanotube field-emission backlight unit [12], and so on, have been reported. In general, the decrease in the response time related to CNTs is due to two main aspects; one is the very strong localized electric field induced by the high length-to-diameter ratio of the CNTs, which is called the electric-field enhancement effect [13], and the other is the strong anchoring between LC molecules and CNTs because of the strong van der Waals interaction [14–17].

The improved relaxation time and the order parameter of a nematic liquid crystal made by using a hybrid alignment mixture of CNTs and polyimide (PI) was reported by Lee [18]. When a hybrid alignment mixture with 1.5-wt.% CNT was used as an alignment layer, the relaxation of the cell was found to be reduced by 35% compared with the value for a cell with a pure PI alignment layer. However, in the hybrid alignment layer, a large number of CNTs will decrease the transpareny and the luminance of the display. Seo [8] demonstrated a LC alignment layer made of ultra-thin single-wall carbon nanotubes (SWNTs) and a conjugated block copolymer nanocomposite, for which the switching time reached approximately 3.8 ms. However, the preparation of ultra-thin SWCNTs is complicated [19–22], and materials that are relatively available are preferred.

Herein, a novel LC alignment layer that is doped with a small number of small SWCNT clusters was prepared in consideration of the facts that the fast switching of twisted nematic liquid crystals (TN-LCs) is caused by the electric-field enhancement effect due to the high length-to-diameter ratio of the SWCNTs and that the anchoring energy between the LCs and the SWCNTs is strong. In addition, the SWCNT clusters outside the surface will effectively reduce the cell gap and will contribute to the fast response of TN-LCs.

II. EXPERIMENTS AND DISCUSSION

For the experiment, all the chemicals and reagents were used as received from commercial sources without any further purification. SWCNTs were obtained from Hanwha Chemical Co., Ltd. The liquid crystal (MAT-04-889) was supplied by Merck Advanced Technology and had a dielectric anisotropy $\Delta\varepsilon = +5.0$ ($\varepsilon_{\parallel} = 8.1$, $\varepsilon_{\perp} = 3.1$), a birefringence $\Delta n = 0.109$ at $\lambda = 589$ nm, $k_1 = 12.3$ pN and $k_3 = 12.8$ pN. The RN-1800 TN alignment layer material was purchased from Nissan Chemical, LTD. For the purification of the SWCNTs, 100 mg of SWCNT powder was sonicated in 100 ml of H_2SO_4/HNO_3 (volume: 3:1) mixture [23–25] at room temperature for 12 h, followed by dilution in 300 ml of distilled (DI) water in an ice bath with stirring. The solution was then centrifuged at 10,000 rpm to separate large bundles of SWCNTs from single SWCNTs and functional SWCNTs. The SWCNTs obtained were washed with DI water until they became neutral; then, they were collected by using a film membrane with the help of a vacuum pump and stored in an oven at 100 °C overnight.

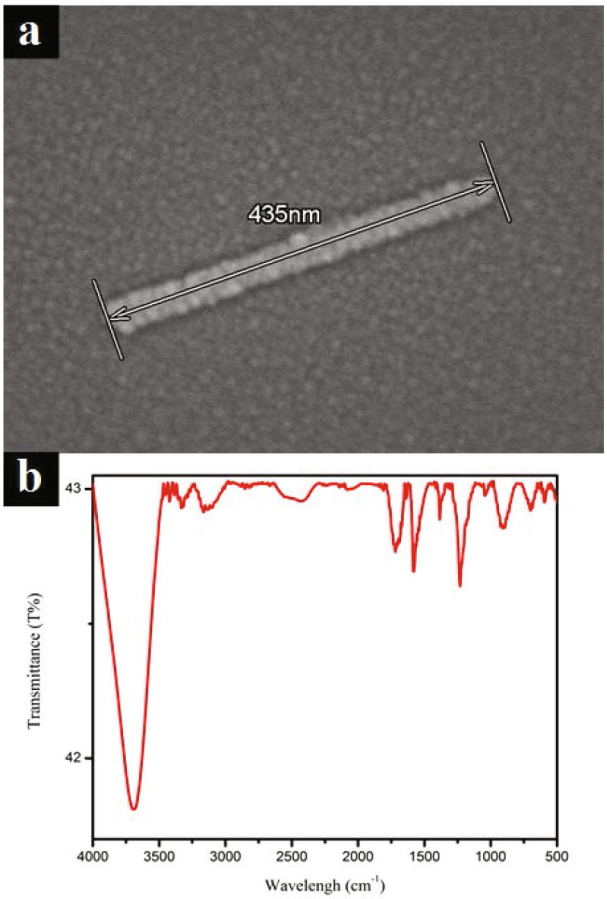

Fig. 1. (Color online) (a) SEM image of a functionalized and cut SWCNT and (b) FT-IR spectrum of a functional SWCNT.

The appearance and functionalization result for the obtained SWCNT is shown in Fig. 1. The functional SWCNTs, 0.02 wt%, were then added to a PI solution to investigate the transparency of the SWCNTs. The mixture was kept in a sonic bath for 4 h at room temperature, followed by a centrifuge process. Thus, a composite with SWCNT clusters randomly dispersed in a PI solution was achieved. The 3-D structures of the clusters were estimated by using a 3-D laser-beam profiler system and atomic force microscopy (AFM, XE-100, PARK System (Korea)).

A typical substrate with a 40-nm-thick indium tin-oxide (ITO) layer was coated with an 80-nm-thick alignment layer. After the alignment layer had been baked under the proper conditions, the surfaces were rubbed by

using a conventional rubbing machine. TN cells were fabricated using those composite, coated and rubbed, ITO substrates. Plastic ball spacers were used to maintain a uniform cell gap (d) of $\sim 3.2 - 3.3$ μm and the optic-electro properties of the LC devices. The nanocomposite alignment layer material was spin-coated on the ITO coated substrates. After the injection of the LCs, the electro-optical properties of the TN cells were measured using an LCMS-200 system (SESIM Photonics Technology).

SWCNTs are an ideal material for the fabrication of optical devices because of their anisotropic intrinsic optical properties, but unfunctionalized SWCNTs have a low dispersion in almost all solvents because of the large van der Waals forces that stacks them together to form large bundles [26]. A high dispersion of SWCNTs can be achieved by adding some aids and by functionalizing with acids or polymers, but the added aids decrease the performances of the composite, and most functionalization processes are complicated and have little effect and low efficiency. Acidification-oxidized SWCNTs can be obtained by sonicating SWCNTs in H_2SO_4/HNO_3 at room temperature, which is easier than other functionalization methods. The neutral-acid-refluxed SWCNTs with -COOH ligands have been proven to be dispersivable in butanol/toluene and xylene/ethanol mixtures, which are poor solvents for pristine SWCNTs [27]. 1, 2-dichorobenzene, chloroform and N-methylpyrrolidinone are the best solvents for dispersing SWCNTs [28].

Figure 1(a) shows characterizations of chopped and functionalized SWCNTs as obtained via field-emission scanning electron microscopy (FE-SEM). The figure shows the SWCNTs appearance and the length of an individual tube. The individual tube has a straight outlook and has a length of about 435 nm, which is 142 times longer than the length of an individual LC molecules. After a 12-h sonication/acid treatment, the -COOH functional group and the -OH functional group were successfully introduced to original SWCNTs, and the length of the original SWCNTs has decreased to less than 500 nm, which contributes to the dispersion of the treated SWCNTs in the composite.

The dispersion and the structure of the SWCNT clusters in the PI alignment layer were confirmed by using optical microscopy (OM) and ultraviolet-visible transmission spectroscopy (UV-vis), as shown in the Fig. 2. These clusters were observed to be randomly located in the composite film, and the sizes of clusters were found to range from nanometers to micrometers. Because of the strong interaction between the SWCNTs and the chemical compatibility between SWCNTs and PI molecules, the SWCNTs in the nanocomposite film existed in clusters rather than as individual SWCNTs. Here, the aggregation of SWCNTs was due to the noneffective functionalization of the SWCNTs, even though a strong acid/sonication treatment had been performed. The noneffective functionalized SWCNTs presented a dispersion property similar to that of the raw nonfunctional CNTs in that they easily form aggregated [29]. The decreased light transmittance of the nanocomposite alignment layer compared with that of the PI alignment layer, as shown in Fig. 2(b), was due to the light absorption of the randomly-located SWCNT clusters.

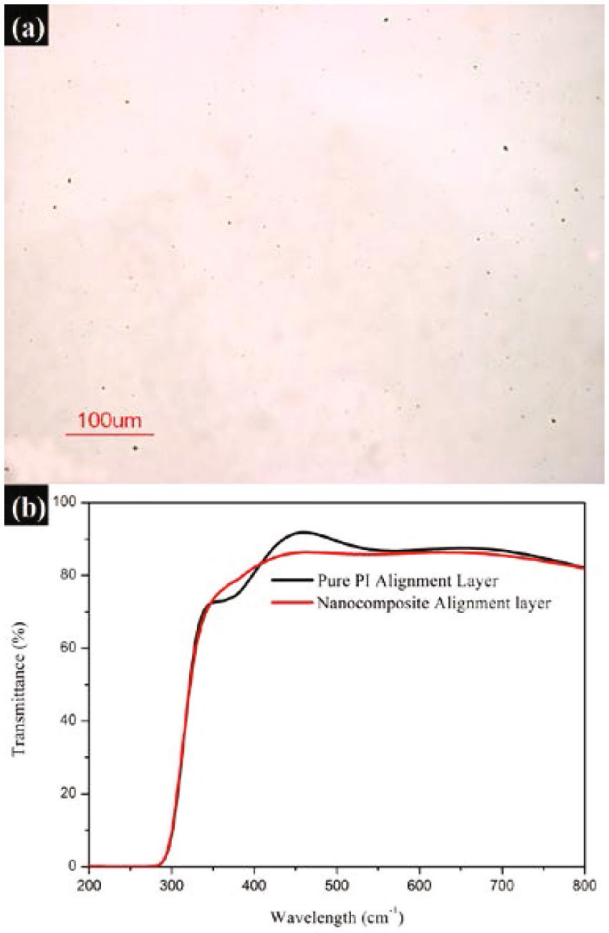

Fig. 2. (Color online) (a) OM image of functionalized and shortened SWCNT clusters doped into a PI alignment layer. (b) Transmittance spectra of a pristine polyimide alignment layer and a nanocomposite alignment layer.

The structures of the SWCNT clusters that had been doped into the PI alignment layer were confirmed by using a 3-D laser-beam profiler and AFM. When such a composite film was exposed to a laser beam of known intensity, some attenuation of the laser light was observed by the analysis system because the light absorptions of the SWCNTs and the PI are different. The composite film was inhomogeneous due to the SWCNT clusters embedded in the polymer layer. In Fig. 3, the clusters and their distributions are clearly observed in both the (b) 2 D image and (c and d) the 3D images. The peaks with different color maps in (d) represent SWCNT clusters with different thicknesses.

The surface morphology of the composite alignment layer was studied by using AFM, and the results are shown in Fig. 4. Clearly, many more clusters like the

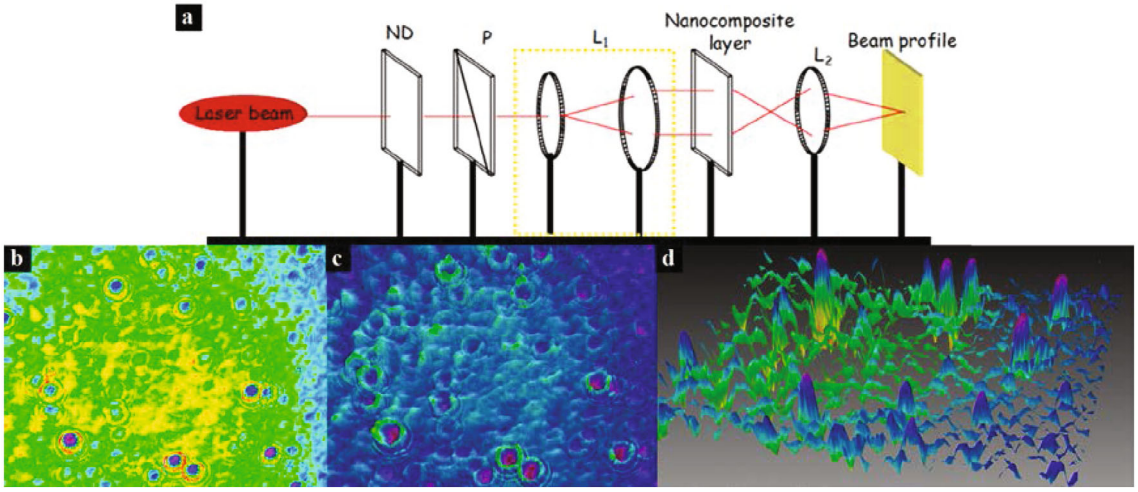

Fig. 3. (Color online) The 3-D topology structure of SWCNT clusters in the PI alignment layer, and confirmed by using a 3-D laser system. (a) The schematic diagram of the 3-D profiler, (b) the 2-D structure of SWCNT clusters, (c) the 3-D structure of SWCNT clusters observed from the right side surface, we usually observe and, (d) 3-D structure of SWCNT clusters observed from the side opposite the one we usually observe.

mountains, exist outside the surface of the nanocomposite alignment layer, and these clusters are concentrated at a height less than 15 nm; the average height of these clusters was found to be about 16.3 nm.

In the TN mode, the normalized transmittance [30] of uniaxial LC molecules between crossed polarizers for the normal white (NW) state is given by

$$T = 1 - \frac{\sin^2[(\pi/2)(1+\mu^2)^{1/2}]}{1+\mu^2}, \qquad (1)$$

where $\mu = 2\Delta \mathrm{nd}/\lambda$, with Δn being the birefringence of the LC, which depends on the voltage, and d and λ being the cell gap and the wavelength of incident light, respectively. To measure the electro-optics properties of a TN cell, we placed the TN cell between crossed polarizer with its rubbing direction parallel to the adjacent polarizer or the analyzer's easy axis. In the field-off state, the LC director remained in a direction different from the transmission axis of the polarizer, and the polarization state of light was changed as it passed through the LC layer; hence, the cell presented a bright state under crossed polarizers. In the presence of an electric field, the vertically aligned LC director tilts, resulting in a decreased effective birefringence of the LC layer, and the cell goes to a dark state. When the CNT clusters exist in a LC medium and the sizes of clusters are larger than 1 μm [31], light leakage has been reported in the dark field-on state. Polarizing optical microscopy (POM) images of a TN cell with a pure PI alignment layer and a TN cell with a composite alignment layer TN cell at voltage-on and voltage-off states are presented in Fig. 5. In the field-off state, several SWCNT aggregates smaller than a micrometer in size were observed while in the field-on state, the composite cell did not exhibit any defects and presented a uniform dark state, just as the TN cell with a pure PI alignment layer did.

The electro-optic performances of the cell with the pure PI alignment layer and the cell with the nanocomposite alignment layer were measured for comparison. The two fabricated test cells were sandwiched between crossed polarizers and were subjected to a continuously increasing voltage (0 V to 9 V) in the form of a 60-Hz square wave with a 0.2-V ramping step. The device was illuminated by using a halogen lamp, and the voltage-dependent transmittance was measured by using a photodiode. As shown in Fig. 6, the transmittance of the cell with the nanocomposite alignment layer is found to lowered by about 4.63% compared to that of the cell with a pure PI alignment layer. The lower light throughput in the case of the cell with the composite material is attributed to the absorption of the CNT clusters present in the composite layer. That enhanced absorption was supported by the decrease in the transmittance that we observed by using visible UV-vis spectroscopy. The voltage to achieve 90% of the total transmittance of the device (V90) for the cell with the nanocomposite alignment layer was 1.924 V, which was larger by about 6.81% compared to the V90 for the cell with the pure PI alignment layer. The voltage to achieve 10% the maximum transmittance of the device (V_{10}), was increased by about 5.02% from 4.237 V in the cell with the pure PI alignment layer to 4.46 V in the cell with the nanocomposite layer. As mentioned in other reports [8], LC cells doped with CNTs and CNT-doped alignment layer have higher driving voltages compared with pure LC cells or cells with pure alignment layers as the elastic constant of the LC composite is different.

The rise time and the decay time of the cell with a pure PI alignment layer and the cell with a nanocomposite alignment layer for eight grey-scale levels caused by an

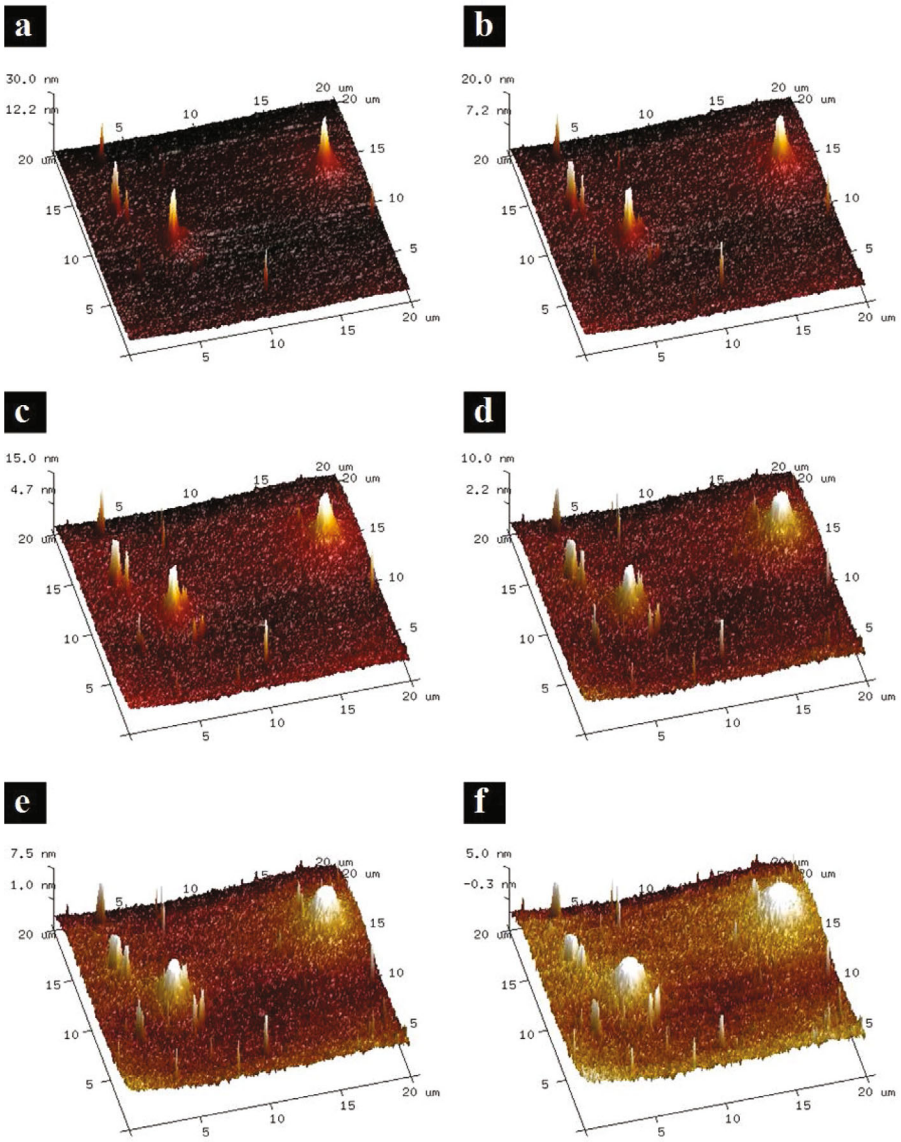

Fig. 4. (Color online) AFM images of the SWCNT clusters outside the surface of the nanocomposite alignment layer at a level approaching or above (a) 30.0 nm, (b) 20.0 nm, (c) 15.0 nm, (d) 10.0 nm, (e) 7.5 nm, (f) 5.0 nm.

60-Hz square-wave voltage are presented in Fig. 7. Significant improvements in the rise time and the decay time were achieved in the cell with the nanocomposite alignment layer, with an average 10.12% faster rise time, an average 29.77% faster decay time, and an average 16.12% faster total response time. A high length-to-diameter ratio can induce a strong local electric field, which is called the electric field enhancement effect. When the concentrated electric field around the SWCNT clusters was exposed to an alternating voltage, the concentrated electric field became strong enough to polarize the LC molecules at a comparatively lower voltage. The strong anchoring between LCs and SWCNTs and the van der-Waals interaction also contributed to the LC's faster response both in the rise time and the decay time. The bumps on the alignment layer's surface are effective in creating an ideal quasi-level support to align LC molecules [32]. Thus, the aligned LCs around the SWCNT clusters in our design induced an alignment of other nearby LCs, and eventually, all LCs were induced to have pre-tilt angles, which contributed to the fast response of the LCs.

The anchoring strength was obtained by using a simple linear fit to the measured phase retardation, R, of the cell with a composite alignment layer in response to an applied voltage, and the results obtained by using the REMS-150 system (SESIM Photonic Technology) are shown in Fig. 8. The following equation [33–35] was used:

$$\frac{R(V-V')}{R_0} = \widetilde{J}_0 - \frac{2k_1}{Wd}(1_k y_p)(V-V'), \qquad (2)$$

where R_0 is the initial phase retardation without an ex-

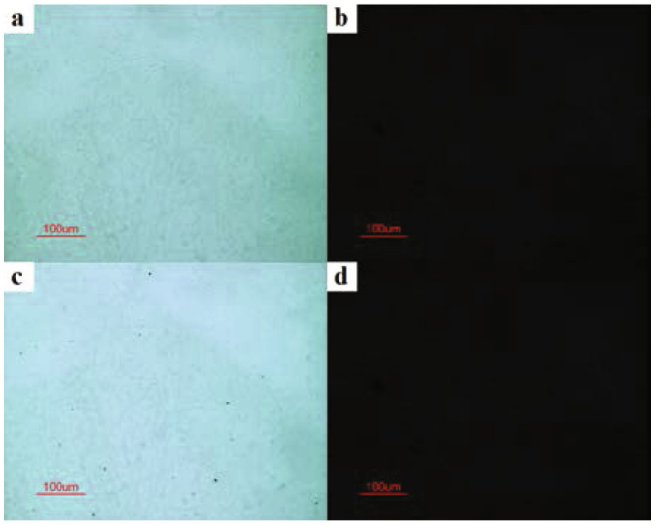

Fig. 5. (Color online) POM images of the (a, c) off- and the (b, d) on-states of a cell with a pure PI alignment layer and a cell with a nanocomposite alignment layer.

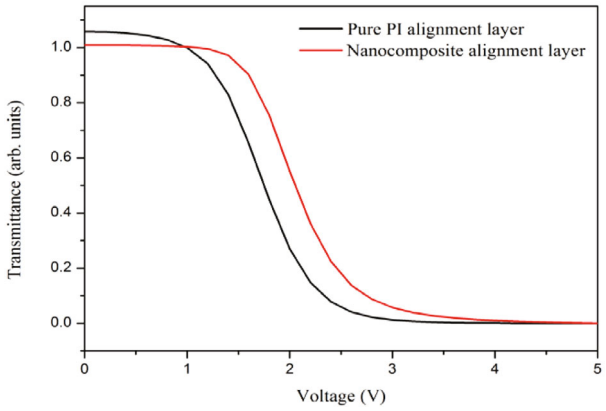

Fig. 6. (Color online) Measured voltage-dependent transmittance curves of a cell with a PI alignment layer and a cell with a nanocomposite alignment layer.

ternal field, and J_0 is the interaction in the X-direction in the plot of $R(V - V')/R_0$ vs. $(V - V')$, $V' = \alpha(1 - \varepsilon_\perp/\varepsilon_\parallel)V_{th}$, W is the polar anchoring strength, $k = (k_3 - k_1)/k_1$, $y_p = \sin 2\theta_p$, and θ_p is the pretilt angle. With a linear fit at voltage above $6V_{th}$, the LCs in the middle layer were parallel to the electric field, and based on the phase-retardation result and the fitted experimented data from $V_{min} = 9.6$ V to $V_{max} = 31.2$ V, the anchoring strength of the cell with a nanocomposite alignment layer was about $W_{nanocomposite} = 3.1066 \times 10^{-3}$ J/m^2, which is much larger than the anchoring strength of the cell with a pure PI alignment layer ($W_{PI} = 4.2538 \times 10^{-4}$ J/m^2). The increased anchoring strength was believed and confirmed to contribute to the fast response of the LCs in the nanocomposite alignment layers.

Faster response also can be achieved by decreasing the

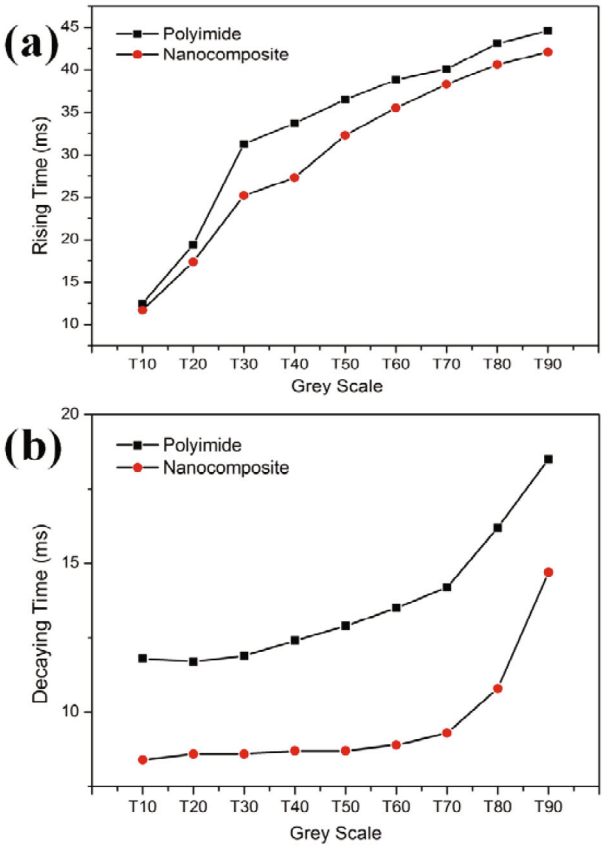

Fig. 7. (Color online) Measured (a) rise and (b) decay response times of a cell with a PI alignment layer and a cell with a nanocomposite alignment layer on a grey scale.

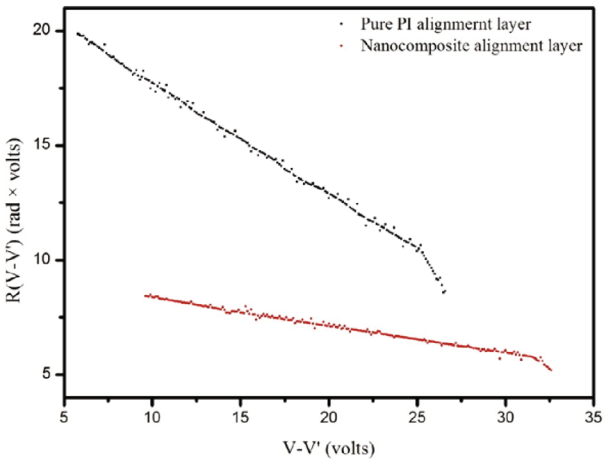

Fig. 8. (Color online) R(V-V') plotted against (V-V').

cell gap. Here, the heights of the SWCNT clusters were taken into consideration, and both the theoretical reduced response time due to the SWCNT clusters, regardless of the localized field enhancement of the SWCNT clusters, and the strong anchoring of LCs on SWCNTs were calculated. As the average height of these clusters

was 16.3 nm, the decrease in cell gap was around 32.6 nm, and the response times at T10 were 24.3 ms and 20.1 ms for the cell with the pure PI alignment layer and the cell with the SWCNT doped PI alignment layer, respectively. The calculated theoretical response time is 24.6 ms for the cell with a SWCNT-cluster-doped layer, but in fact, the measured response time is 20.1 ms, which is a decrease of 4.5 ms and indicates that the faster response may be caused by the decreased cell gap. The decrease of 4.5 ms in the response time is also evidence that the localized field enhancement due to the SWCNT clusters and the strong anchoring of LCs on SWCNTs also contributes to the decreased time.

III. CONCLUSION

A 3-D SWCNT cluster-doped PI alignment layer was achieved, and the morphology of the composite film was confirmed by using OM images, 3-D laser profile images and AFM images. The TN cell fabricated with a composite alignment layer showed a slight decrease in the transmittance due to the SWCNT clusters, but a superfaster response time. The faster response time was attributed to the electric-field enhancement effect caused by the SWCNT clusters, the strong anchoring strength between the LC and the SWCNT clusters, the decrease in the effective cell gap, and the bumps on the alignment layer's surface. Hence, the presented experimented result showed the possibility for new applications of LCDs that have SWCNT clusters in their alignment layers.

ACKNOWLEDGMENTS

This work was supported by the Basic Research Laboratory Program (2014R1A4A1008140) through the Ministry of Science, ICT & Future Planning and by the Basic Scie nce Research Program through the National Research Foundation of Korea (NRF) funded by the Ministry of Education (2014R1A1A2004467).

REFERENCES

[1] M. Nagaraj, V. Görtz, J. W. Goodby and H. F. Gleeson, Appl Phys. Lett. **104**, 021903 (2014).
[2] S. H. Lee, S. S. Bhattacharyya, H. S. Jin and K. U. Jeong, J. Mater. Chem. **22**, 11893 (2012).
[3] H. Kikuchi, M. Yokota, Y. Hisakado, H. Yang and T. Kajiyama, Nat. Mater. **1**, 64 (2002).
[4] T.-Z. Shen, S.-H. Hong and J.-K. Song, Nat. Mater. **13**, 394 (2014).
[5] Y. Hisakado, H. Kikuchi, T. Nagamura and T. Kajiyama, Adv. Mater. **17**, 96 (2005).
[6] Z. Ge, S. Gauza, M. Jiao, H. Xianyu and S-T. Wu, Appl. Phys. Lett. **94**, 101104 (2009).
[7] C. Escher and R. Wingen, Adv. Mater. **4**, 189 (1992).
[8] W.-K. Lee, Y. S. Choi, Y.-G. Kang, J. Sung, D.-S. Seo and C. Park, Adv. Funct. Mater. **21**, 3843 (2011).
[9] H.-Y. Chen, W. Lee and N. A. Clark, Appl. Phys. Lett. **90**, 033510 (2007).
[10] R. Basu, R. G. Petschek and C. Rosenblatt, Phys. Rev. E **83**, 041707 (2011).
[11] Y. S. Ha, H. J. Kim, H. G. Park and D. S. Seo, Opt. Express **6**, 6448 (2012).
[12] Y. C. Choi *et al.*, Nanotechnology **19**, 235306 (2008).
[13] W. Fu, Z. Xu, X. Bai, C. Gu and E. Wang, Nano Lett. **9**, 921 (2009).
[14] H. Qi and T. Hegmann, J. Mater. Chem. **18**, 3288 (2008).
[15] J. P. F. Lagerwall and G. Scalia, J. Mater. Chem. **18**, 2890 (2008).
[16] H. Qi, B. Kinkead and T. Hegmann, Adv. Funct. Mater. **18**, 212 (2008).
[17] J. Lagerwall, G. Scalia, M. Haluska, U. Dettlaff-Weglikowska, S. Roth and F. Giesselmann, Adv. Mater. **19**, 359 (2007).
[18] H. Lee, S. Yang, J.-H. Lee and Y. S. Park, Appl. Phys. Lett. **104**, 191601 (2014).
[19] G.-H. Jeong, A. Yamazaki, S. Suzuki, H. Yoshimura, Y. Kobayashi and Y. Homma, J. Am. Chem. Soc. **127**, 8238 (2005).
[20] H. Qi, C. Qian and J. Liu, Nano Lett. **7**, 2417 (2007).
[21] J. Zhang, Y. Yan, M. W. Chance, J. Chen, J. Hayat, S. Ma and C. Tang, Angew. Chem. **125**, 13629 (2013).
[22] Y. Zou, Q. Li, J. Liu, Y. Jin. Y. Liu, Q. Qian, K. Jiang and S. Fan, Appl. Phys. Express **7**, 055102 (2014).
[23] Y. Zhang, Z. Shi, Z. Gu and S. Iijima, Carbon **38**, 2055 (2000).
[24] Z. Jia, Z. Wang, J. Liang, B. Wei and D. Wu, Carbon **37**, 903 (1999).
[25] J. Liu *et al.*, Science **280**, 1253 (1998).
[26] L. Hu, D. S. Hecht and G. Grüner, Chem. Rev. **110**, 5790 (2010).
[27] J. Y. Lee, K. Liang, K. H. An and Y. H. Lee, Synth. Met. **150**, 153 (2005).
[28] J. L. Bahr, E. T. Mickelson, M. J. Bronikowski, R. E. Smalley and J. M. Tour, Chem. Commun. 193 (2001).
[29] B. K. Zhu, S. H. Xie, Z. K. Xu and Y. Y. Xu. Compos. Sci. Tech. **66**, 548 (2006).
[30] S. J. Jeong, K. A. Park, S. H. Jeong, H. J. Jeong, K. H. An, C. W. Nah, D. Pribat, S. H. Lee and Y. H. Lee. Nano Lett. **7**, 2178 (2007).
[31] Y. J. Lim, S. S. Bhattacharyya, W. Tie, H. R. Park, Y. H. Lee and S. H. Lee. Liq. Cryst. **40**, 1202 (2013).
[32] W. Zhou, L. J. Lin, D. Y. Zhao and L. Guo. J. Am. Chem. Soc. **133**, 8389 (2011).
[33] Yu. A. Nastishin, R. D. Polak, S. V. Shiyanovskii and O. D. Lavrentovich, Appl. Phys. Lett. **75**, 202 (1999).
[34] S.-Y. Lu and L.-C. Chien, Opt. Express **16**, 12777 (2008).
[35] X. Nie, R. Lu, H. Xianyu, T. X. Wu and S.-T. Wu, J. Appl. Phys. **101**, 103110 (2007).